77°K. In Fig. 7, G at 77°K has been plotted against p^2 and appears to be a linear function of p^2. In order to make the curve meet the origin, the constant 17 sec^{-1} has been subtracted from G. The possibility that this constant term represents the loss of metastable atoms resulting from "forbidden" radiation has been discussed above.

Molnar[7] has pointed out that "since rates of electron diffusion or recombination depend on gas temperature in a not very sensitive way, it may be possible to separate the destructive effects of these particles from those of the neutral atoms by careful measurements of G as a function of temperature and pressure." Since the $^3P_2$ metastable level is 0.05 ev lower than the radiating $^3P_1$ level, the probability of this transition, on the other hand, should be highly dependent on the kinetic energy of the colliding particles, i.e., on the gas temperature.

According to this interpretation, we should expect that the dominant process at 77°K is not destruction of metastables by collisions with normal atoms. Inspection of the experimental results (Fig. 5) leads us to believe that the less temperature-sensitive process introduces into G a term proportional to p^2. The shape of the curves suggests that if measurements were made at pressures above 20 mm of mercury, this process would probably be the dominant one at all the temperatures considered.

The authors wish to thank Professor R. D. Myers for much stimulating discussion of the results obtained in this research.

[7] J. P. Molnar, Bell Telephone Laboratories Report 38140 (July 18, 1950) (unpublished).

PHYSICAL REVIEW VOLUME 90, NUMBER 1 APRIL 1, 1953

The Photodisintegration of the Deuteron

LAMEK HULTHÉN AND BENGT C. H. NAGEL
Royal Institute of Technology, Stockholm, Sweden

(Received December 3, 1952)

The photomagnetic and photoelectric cross sections have been calculated for γ-energies from threshold (2.23 Mev) up to 20 Mev, using a central Yukawa potential with the same range (i.e., meson mass) in the ^1S and ^3S states and no interaction in the ^3P state. Exchange and quadrupole effects have been neglected. Results are given for three ranges, equivalent to meson masses 199, 256, and 298.5, and are compared with recent measurements.

In the last section a comparison is made with the results obtained by the effective range method.

I. INTRODUCTION

In two previous papers[1,2] by Hansson and one of the present authors, theoretical values of the photo cross sections were given for a few γ-energies (2.52, 2.62, 2.76, and 6.20 Mev). We have found it desirable to extend these calculations to the whole region of small and moderate energies, at the same time trying to improve the accuracy. On the other hand, the underlying theoretical assumptions have been simplified in some respects. Thus we have neglected the influence of the charge exchange on the photomagnetic cross section σ_m, mainly because it is difficult to find an unambiguous basis for treating this effect. It should also be pointed out that the effect has been calculated in the case of the Møller-Rosenfeld theory where it turned out to be insignificant.[1,3] Moreover, we have carried out the present calculations of the photoelectric cross section σ_e on the assumption that no interaction exists in the ^3P state. The earlier results[1,2] indicate that σ_e is not very sensitive to variations of the ^3P interaction within plausible limits. A closer study of this point is deferred to a forthcoming paper by Hansson.

[1] I. F. E. Hansson and L. Hulthén, Phys. Rev. **76**, 1163 (1949).
[2] I. F. E. Hansson, Phys. Rev. **79**, 909 (1950).
[3] See also B. C. H. Nagel and S. G. Nilsson, Transactions of the Royal Institute of Technology (to be published).

Thus we have assumed the following interactions:

$$\begin{aligned} &^1S: \quad V(r)=-{}^1B\cdot e^{-\kappa r}/r, \\ &^3S: \quad V(r)=-{}^3B\cdot e^{-\kappa r}/r, \\ &^3P: \quad V(r)=0, \\ &\kappa=M_m c/\hbar, \quad M_m \text{ meson mass.} \end{aligned} \tag{1}$$

The calculations have been carried out for three different ranges $1/\kappa$, corresponding to meson masses 199.0, 255.8, and 298.5 M_e (electron mass). In each case ^3B has been determined from the deuteron binding energy $|E_0|$, for which we have accepted the value 2.23 Mev. ^1B is then fixed by the epithermal neutron-proton scattering cross section $\sigma_0=20.36$ barns, taking into account that the ^1S state is virtual.

II. CALCULATION OF THE EIGENFUNCTIONS

Introducing dimensionless quantities, the Schrödinger equation of an S state can be reduced to the following form, $\phi(x)$ being proportional to r times the radial part $\psi(r)$ of the wave function:

$$d^2\phi/dx^2+\left(a+b\frac{e^{-x}}{x}\right)\phi=0, \tag{2}$$

where $x=\kappa r$, $a=M(E/\hbar^2\kappa^2)$, $M=\frac{1}{2}(M_n+M_p)$, ($E=$ en-

TABLE I. Approximate ground-state functions for three different meson masses M_m/M_e. The symbols used are explained in the text.

$(-a_0)^{\frac{1}{2}}$	^3b	h_1	h_2	h_3	C	$(1/\kappa)\times10^{+13}$ (cm)	M_m/M_e	^1b
0.45	2.6629	0.63898	−0.10108	0.06347	1.37296	1.9408	199.0	1.5071
0.35	2.4490	0.63657	−0.11379	0.06877	1.13166	1.5095	255.8	1.5436
0.30	2.3413	0.63514	−0.12084	0.07181	1.01048	1.2939	298.5	1.5624

ergy in the center-of-mass system, M_n=neutron mass, M_p=proton mass), and $b=MB/\hbar^2\kappa$.

For the eigenfunction of the ground state we have used the results of Hulthén and Laurikainen.[4] Taking

$$\phi_0(x)=C\exp[-(-a_0)^{\frac{1}{2}}x](1-e^{-x})\times(1+h_1e^{-x}+h_2e^{-2x}+h_3e^{-3x}),\qquad \int_0^\infty\phi_0^2dx=1, \tag{3}$$

we get the values of the parameters given in Table I.

The eigenfunctions of the continuous ^1S spectrum have been obtained by the method described by Hulthén.[5] The form of the trial function is

$$\phi_1(x)=\sin(a^{\frac{1}{2}}x+\eta)-\sin\eta[e^{-x}+(1-e^{-x})\times(c_1e^{-x}+c_2e^{-2x}+c_3e^{-3x})], \tag{4}$$

η being the asymptotic phase. Thus ϕ_1 is normalized to amplitude 1 for $x\to\infty$. The ^1b values are found in Table I.

The approximate solutions (4) are given in Table II for some values of $a^{\frac{1}{2}}$. A more detailed account of these calculations is given by Hulthén and Skavlem.[6]

We also write down the eigenfunction of the ^3P state, corresponding to interaction zero,

$$\phi_2(x)=\frac{\sin(a^{\frac{1}{2}}x)}{a^{\frac{1}{2}}x}-\cos(a^{\frac{1}{2}}x). \tag{5}$$

III. FORMULAS FOR THE CROSS SECTIONS

Using the preceding notations, the cross section for the photoelectric dipole transition from the ground state to a ^3P state can be expressed as follows:

$$\sigma_e=\frac{\pi}{3}\frac{e^2}{\hbar c}\left(\frac{M_n}{M_m}\right)^2\frac{1}{\kappa^2}\frac{h\nu}{Mc^2}\frac{1}{a^{\frac{1}{2}}}J_e^2,\qquad J_e=\int_0^\infty\phi_0(x)\phi_2(x)x\,dx, \tag{6}$$

a being connected with the γ-energy $h\nu$ and the binding energy $|E_0|$ in the following way:

$$a=\frac{M}{\hbar^2\kappa^2}\left(h\nu-|E_0|-\frac{(h\nu)^2}{4Mc^2}\right); \tag{7}$$

the last term (the Doppler effect) is negligible in the energy region considered here.

The corresponding expression for the photomagnetic cross section ($^3S\to{}^1S$) is

$$\sigma_m=\frac{\pi}{3}\frac{e^2}{\hbar c}(\mu_p-\mu_n)^2\left(\frac{M}{M_p}\right)^2\frac{1}{\kappa^2}\frac{h\nu}{Mc^2}\frac{1}{a^{\frac{1}{2}}}J_m^2,\qquad J_m=\int_0^\infty\phi_0(x)\phi_1(x)dx, \tag{8}$$

where μ_p and μ_n are the magnetic moments of proton and neutron, respectively, expressed in nuclear magnetons ($e\hbar/2M_pc$): $\mu_p=2.7928$, $\mu_n=-1.9131$.

In each case J_m has been obtained for the proper ^1b value (Table I) by quadratic interpolation between the J_m values corresponding to the b's of Table II.

IV. A METHOD FOR IMPROVING THE VALUES OF THE MATRIX ELEMENTS

In order to get an idea of the accuracy of the matrix elements, we carried out the calculation in a few cases, using approximate eigenfunctions with one, two, and three parameters, respectively.

By way of illustration, take the case of the photoelectric matrix element J_e for $h\nu=4.46$ Mev and $M_m=298.5M_e$ [$(-a_0)^{\frac{1}{2}}=0.3$, $a^{\frac{1}{2}}=0.3$]. Table III gives

TABLE II. Approximate ^1S state eigenfunctions. The symbols used are explained in the text.

b	$a^{\frac{1}{2}}$	c_1	c_2	c_3	$\cot\eta$
1.50	→0	−0.5430	0.1864	−0.0995	$0.086117/(a)^{\frac{1}{2}}$
1.55	→0	−0.5673	0.1899	−0.1026	$0.060676/(a)^{\frac{1}{2}}$
1.60	→0	−0.5922	0.1930	−0.1056	$0.036455/(a)^{\frac{1}{2}}$
1.50	0.1	−0.5645	0.2081	−0.1108	0.98346
1.55	0.1	−0.5887	0.2113	−0.1138	0.72404
1.60	0.1	−0.6134	0.2135	−0.1162	0.47707
1.50	0.2	−0.6245	0.2668	−0.1408	0.67102
1.55	0.2	−0.6481	0.2679	−0.1426	0.53399
1.60	0.2	−0.6723	0.2686	−0.1442	0.40356
1.50	0.3	−0.7119	0.3458	−0.1795	0.68863
1.55	0.3	−0.7349	0.3445	−0.1799	0.53953
1.60	0.3	−0.7584	0.3426	−0.1802	0.44524
1.50	0.4	−0.8147	0.4283	−0.2168	0.66982
1.55	0.4	−0.8363	0.4223	−0.2145	0.58786
1.60	0.4	−0.8588	0.4172	−0.2130	0.50990
1.50	0.5	−0.9201	0.4924	−0.2389	0.72164
1.55	0.5	−0.9416	0.4857	−0.2368	0.64872
1.60	0.5	−0.9632	0.4777	−0.2340	0.57941

[4] L. Hulthén and K. V. Laurikainen, Revs. Modern Phys. **23**, 1 (1951).
[5] L. Hulthén, Arkiv Mat. Astron. Fysik **A35**, No. 25 (1948).
[6] L. Hulthén and S. Skavlem, Phys. Rev. **87**, 297 (1952).

TABLE III. Ground-state functions with one, two, and three parameters [Eq. (3)] and corresponding photoelectric matrix elements $(J_e)_n$. $(-a_0)^{\frac{1}{2}}=0.3$; $(a)^{\frac{1}{2}}=0.3$; ${}^3b=2.3413$.

n	h_1	h_2	h_3	C_n	C_n/C_3	$(J_e)_n$	$(J_e)_n/(J_e)_3$	I_∞
1	0.57430	...	...	1.01535	1.00482	5.61265	1.00435	0.98963
2	0.59356	−0.01953	...	1.01333	1.00282	5.60238	1.00251	0.99240
3	0.63414	−0.12084	0.07181	1.01048	1.00000	5.58833	1.00000	0.99596
		Extrapolated to $I_\infty=1$		1.00745	0.99700	5.5730	0.99725	1.00000

the values of the parameters obtained by Hulthén and Laurikainen[4] and the corresponding J_e. I_∞ is an integral, defined by[7]

$$I_\infty=\frac{{}^3b}{C(-a_0)^{\frac{1}{2}}}\int_0^\infty \sinh[(-a_0)^{\frac{1}{2}}x]\frac{e^{-x}}{x}\phi_0(x)dx. \quad (9)$$

This quantity would equal 1 if $\phi_0(x)$ were exact;[8] the deviation from 1 gives an idea of the accuracy of $\phi_0(x)$ preferably at large and moderate x.

Table III indicates a correlation between J_e and the normalization constant $C(=C_n)$. This is not surprising; for small and moderate energies J_e is largely determined by the asymptotic behavior of $\phi_0(x)$, that is $C\exp[-(-a_0)^{\frac{1}{2}}x]$. This, however, does not help us so much, since we do not know the correct value of C, corresponding to an infinite number of parameters. But there is also reason to expect a correlation of C with I_∞. C is determined from the parameters h_ν by the condition [see Eq. (3)]

$$I_N=\int_0^\infty\left(\frac{\phi_0(x)}{C}\right)^2dx=\frac{1}{C^2};$$

and, plotting I_N or C against I_∞, we get a fairly straight line. Extrapolating to $I_\infty=1$, we obtain a C value, which should represent the asymptotic behavior of $\phi_0(x)$ more correctly, $C_{\text{extr}}=1.00745$. This would give us a possibility to improve J_e, but we prefer to do this by plotting J_e directly against I_∞ (see Fig. 1). Extrapolation to $I_\infty=1$ gives $(J_e)_{\text{extr}}=0.9972_5\cdot(J_e)_3=5.5730$. The correction factors were calculated in this way for a few instances, most of which are given in Table IV. In other cases the correction factors can be obtained by linear interpolation.

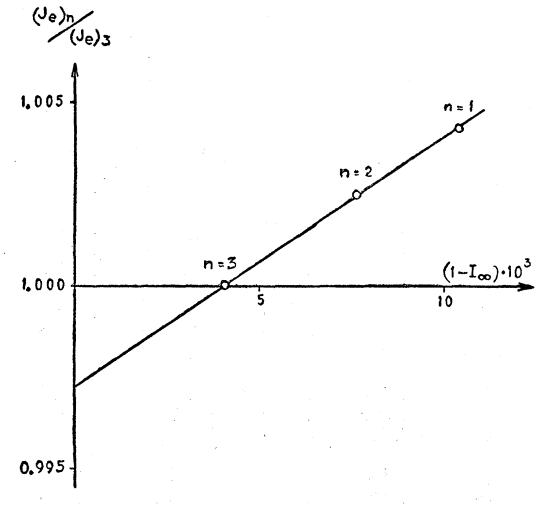

FIG. 1. Correction of the photoelectric matrix element.

The same procedure can be applied to the integral J_m as far as the error arising from $\phi_0(x)$ is concerned. It is also possible to correct for the uncertainty from $\phi_1(x)$ in a similar way, by plotting J_m, calculated with one, two, and three parameters c_ν [Eq. (4)] and three parameters h_ν in $\phi_0(x)$ against the integral

$$\rho_1=\frac{{}^1b\cdot\int_0^\infty \sin(a^{\frac{1}{2}}x)\cdot\frac{e^{-x}}{x}\phi_1(x)dx}{a^{\frac{1}{2}}\sin\eta}, \quad (10)$$

which would equal 1 for an exact solution $\phi_1(x)$.[9] An example is given in Table V. [For $\phi_0(x)$ see Table I.]

Since the corrections turn out to be small, it seems safe to assume that the errors due to $\phi_0(x)$ and $\phi_1(x)$ add linearly. The total correction thus obtained is given in Table VI for a few cases.

TABLE IV. Correction factors for the photoelectric matrix element J_e. To obtain an improved J_e value, multiply $(J_e)_3$ [three parameters in $\phi_0(x)$] by the correction factor given below.

	$h\nu$ (in Mev)				
$(-a_0)^{\frac{1}{2}}$	2.23	4.46	6.14	10.00	15.00
0.30	0.9970	0.9973	0.9975	0.9977	0.9986
0.45	0.9962	0.9968	0.9975	0.9994	1.0000

TABLE V. ^1S state eigenfunctions with one, two, and three parameters and corresponding photomagnetic matrix element $(J_m)_n$. $(-a_0)^{\frac{1}{2}}=0.45$; ${}^1b=1.5$; $a=0$.

n	c_1	c_2	c_3	$a^{\frac{1}{2}}\cot\eta$	ρ_1	$\frac{J_m}{(a)^{\frac{1}{2}}}$	$\frac{(J_m)_n}{(J_m)_3}$
1	−0.4633	...	...	0.086200	0.9951	29.359	0.99594
2	−0.5074	0.0644	...	0.086134	0.9980	29.444	0.99884
3	−0.5430	0.1864	−0.0995	0.086117	0.9991	29.478	1.00000
			Extrapolated to $\rho_1=1$			29.505	1.0009

[7] In the corresponding formula (22) of reference 4, h_ν should be replaced by h_ν/h_0.

[8] L. Hulthén, Kgl. Fysiograf. Sällskap. Lund, Förh. **15**, No. 22 (1945).

[9] L. Hulthén, Kgl. Fysiograf. Sällskap. Lund, Förh. **14**, No. 8 (1944).

TABLE VI. Correction factors for the photomagnetic matrix element J_m. To obtain an improved J_m value, multiply $(J_m)_3$ [three parameters in $\phi_0(x)$ as well as in $\phi_1(x)$] by the correction factor given below.

$(-a_0)^{\frac{1}{2}}$	$h\nu$ (in Mev) 2.23	2.34	2.48
0.30	0.9993	···	0.9995
0.45	0.9994	0.9996	···

V. RESULTING CROSS SECTIONS

The resulting values for σ_m, σ_e, etc., are given in Tables VII to X.[10] The remaining uncertainty resulting from errors in the eigenfunctions is believed not to exceed one or two parts in a thousand.

For the sake of completeness we also include, in Table X, the results of earlier calculations[3,11] of the neutron-proton capture cross section σ_c.

Figures 2–6 give the results in graphical form. In the graphs for σ and σ_m/σ_e, the theoretical curves are compared with some recent experimental results. These experimental values are also given in the captions of the figures together with the corresponding theoretical values, interpolated to a meson mass $286.4M_e$. This meson mass is fixed by the coherent scattering amplitude $f=-3.78\times10^{-13}$ cm[12] (see Sec. VIIIA).

TABLE VII. Resulting photo cross sections, $(-a_0)^{\frac{1}{2}}=0.30$; $M_m/M_e=298.5$. Cross sections are given in units of 10^{-28} cm². $\sigma=\sigma_m+\sigma_e$. Figures in brackets indicate uncertain interpolation.

$a^{\frac{1}{2}}$	$h\nu$ (Mev)	σ_m	σ_e	σ	σ_m/σ_e
0.01	2.232	(2.13)	0.007	2.14	300
0.02	2.240	(3.80)	0.056	3.86	68
0.03	2.252	(4.83)	0.186	5.02	26
0.04	2.270	(5.33)	0.432	5.76	12.3
0.05	2.292	5.440	0.819	6.26	6.640
0.06	2.319	5.315	1.366	6.68	3.890
0.08	2.389	4.769	2.964	7.73	1.609
0.10	2.478	4.131	5.185	9.32	0.7967
0.12	2.587	3.542	7.873	11.41	0.4498
0.14	2.716	3.034	10.804	13.84	0.2808
0.15	2.788	2.811	12.284	15.10	0.2288
0.16	2.864	2.606	13.740	16.35	0.1897
0.18	3.033	2.247	16.473	18.72	0.1364
0.20	3.221	1.946	18.853	20.80	0.1032
0.25	3.779	1.385	22.777	24.16	0.0608
0.30	4.460	1.011	23.883	24.89	0.0423
0.35	5.265	0.756	22.977	23.73	0.0329
0.40	6.195	0.578	20.976	21.55	0.0276
0.45	7.248	0.451	18.553	19.00	0.0243
0.50	8.425	0.357	16.104	16.46	0.0221
0.55	9.725	0.287	13.829	14.12	0.0208
0.60	11.150	0.234	11.810	12.04	0.0198
0.65	12.699	0.193	10.064	10.26	0.0191
0.70	14.371	0.161	8.573	8.73	0.0187
0.75	16.168	0.136	7.311	7.45	0.0186
0.80	18.088	0.116	6.246	6.36	0.0186
0.90	22.300	0.082	4.591	4.67	0.0179
1.00	27.008	0.062	3.411	3.47	0.0182

TABLE VIII. Resulting photo cross sections. $(-a_0)^{\frac{1}{2}}=0.35$; $M_m/M_e=255.8$. Cross sections are given in units of 10^{-28} cm².σ $=\sigma_m+\sigma_e$. Figures in brackets indicate uncertain interpolation.

$a^{\frac{1}{2}}$	$h\nu$ (Mev)	σ_m	σ_e	σ	σ_m/σ_e
0.01	2.232	(1.77)	0.005	1.78	370
0.02	2.237	(3.28)	0.038	3.32	86
0.03	2.246	(4.37)	0.127	4.50	34
0.04	2.259	(5.03)	0.296	5.33	17.0
0.05	2.276	5.332	0.566	5.90	9.428
0.06	2.296	5.371	0.952	6.32	5.643
0.07	2.319	5.258	1.466	6.72	3.588
0.08	2.347	5.052	2.112	7.16	2.392
0.10	2.412	4.530	3.797	8.33	1.193
0.12	2.492	3.991	5.947	9.94	0.6711
0.14	2.587	3.499	8.442	11.94	0.4144
0.15	2.640	3.275	9.771	13.05	0.3352
0.16	2.696	3.067	11.127	14.19	0.2757
0.18	2.820	2.695	13.840	16.53	0.1947
0.20	2.958	2.374	16.435	18.81	0.1444
0.25	3.368	1.755	21.717	23.47	0.0808
0.30	3.868	1.325	24.704	26.03	0.0536
0.35	4.460	1.018	25.517	26.53	0.0399
0.40	5.143	0.798	24.754	25.55	0.0322
0.45	5.916	0.635	23.042	23.68	0.0275
0.50	6.781	0.511	20.869	21.38	0.0245
0.55	7.737	0.417	18.569	18.99	0.0225
0.60	8.784	0.344	16.339	16.68	0.0211
0.65	9.921	0.286	14.277	14.56	0.0201
0.70	11.150	0.241	12.428	12.67	0.0194
0.75	12.470	0.206	10.797	11.00	0.0191
0.80	13.881	0.176	9.375	9.55	0.0188
0.90	16.976	0.128	7.078	7.21	0.0181
1.00	20.434	0.097	5.364	5.46	0.0182

TABLE IX. Resulting photo cross sections. $(-a_0)^{\frac{1}{2}}=0.45$; $M_m/M_e=199.0$. Cross sections are given in units of 10^{-28} cm².σ $=\sigma_m+\sigma_e$. Figures in brackets indicate uncertain interpolation.

$a^{\frac{1}{2}}$	$h\nu$ (Mev)	σ_m	σ_e	σ	σ_m/σ_e
0.01	2.231	(1.30)	0.003	1.31	510
0.02	2.234	(2.59)	0.021	2.62	127
0.03	2.240	(3.63)	0.069	3.70	53
0.04	2.248	(4.37)	0.161	4.53	27.1
0.05	2.258	4.860	0.310	5.17	15.66
0.06	2.270	5.126	0.528	5.65	9.715
0.08	2.300	5.200	1.201	6.40	4.331
0.10	2.340	4.945	2.227	7.17	2.220
0.12	2.389	4.564	3.619	8.18	1.261
0.14	2.446	4.156	5.350	9.51	0.7768
0.15	2.478	3.956	6.328	10.28	0.6253
0.16	2.512	3.764	7.369	11.13	0.5108
0.18	2.587	3.405	9.602	13.01	0.3546
0.20	2.671	3.081	11.964	15.04	0.2575
0.25	2.918	2.412	17.872	20.28	0.1350
0.30	3.221	1.921	22.911	24.83	0.0838
0.35	3.579	1.547	26.437	27.98	0.0585
0.40	3.992	1.261	28.329	29.59	0.0445
0.45	4.460	1.039	28.787	29.83	0.0361
0.50	4.983	0.864	28.160	29.02	0.0307
0.55	5.561	0.725	26.793	27.52	0.0271
0.60	6.195	0.613	24.983	25.60	0.0246
0.65	6.883	0.522	22.964	23.49	0.0227
0.70	7.626	0.447	20.885	21.33	0.0214
0.75	8.425	0.385	18.854	19.24	0.0204
0.80	9.278	0.333	16.928	17.26	0.0197
0.90	11.150	0.254	13.503	13.76	0.0188
1.00	13.243	0.197	10.698	10.90	0.0185

[10] For the fundamental constants entering into Eqs. (6)–(8) we have used the following figures: $\hbar c/e^2=137.04$; $Mc^2=938.8$ Mev; $M_n/M_p=1.00138$; $h=6.6237\times10^{-27}$ erg; $M_p/M_e=1836.0$. The deviations of these values from those given by J. A. Bearden and H. M. Watts, Phys. Rev. **81**, 73 (1951) are insignificant in this connection.

[11] L. Hulthén, Phys. Rev. **79**, 166 (1950).

[12] Ringo, Burgy, and Hughes, Phys. Rev. **82**, 344 (1951).

TABLE X. Neutron-proton capture cross section σ_c at a neutron velocity of 2.2×10^5 cm/sec, $|E_0|=2.23$ Mev.

M_m/M_e	σ_c (barns)
200	0.3013
300	0.3089
286.4	0.3079

VI. ANGULAR DISTRIBUTION IN THE LABORATORY SYSTEM

If the values of σ_m/σ_e are to be compared with results obtained from measurements on the angular distribution of photoneutrons (or protons), the influence of the γ-ray momentum must normally be taken into account. Let θ be the angle between the directions of the photoneutron and the incident γ-ray, respectively, in the laboratory system (deuteron initially at rest). Simple geometrical considerations then give the following differential cross section $\sigma(\theta)$ in the laboratory system:

$$\sigma(\theta)d\Omega=(\sigma_m+\tfrac{3}{2}\sigma_e\sin^2\theta f(\theta))\times(1-\alpha^2\sin^2\theta)^{-\frac{1}{2}}f(\theta)d\Omega/4\pi,$$
$$f(\theta)=1+2\alpha\cos\theta(1-\alpha^2\sin^2\theta)^{\frac{1}{2}}+\alpha^2(\cos^2\theta-\sin^2\theta),\qquad(11)$$
$$\alpha=\bar{v}/v_n.$$

Here $\bar{v}$ is the velocity of the center of mass of the neutron and proton in the laboratory system and v_n is the velocity of the neutron relative to the center of mass; thus,

$$\frac{\bar{v}}{v_n}=\frac{h\nu}{2[(MM_p/M_n)c^2\{h\nu-|E_0|-(h\nu)^2/4Mc^2\}]^{\frac{1}{2}}},\qquad(12)$$

where M_n and M_p denote the masses of the neutron and proton, respectively.

VII. DISCUSSION

For a comparison with experimental results we refer to Figs. 4–6. The most accurate determinations of the

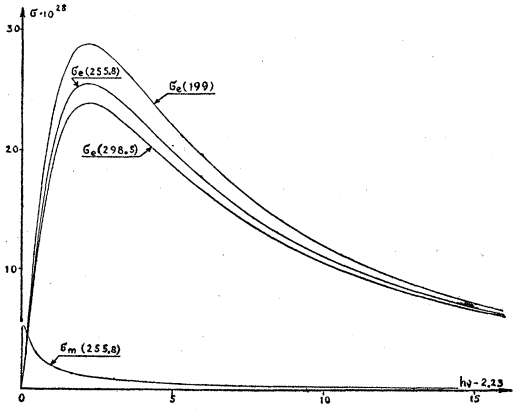

FIG. 2. The photoelectric cross section as a function of excess energy $h\nu-2.23$. Three meson masses.

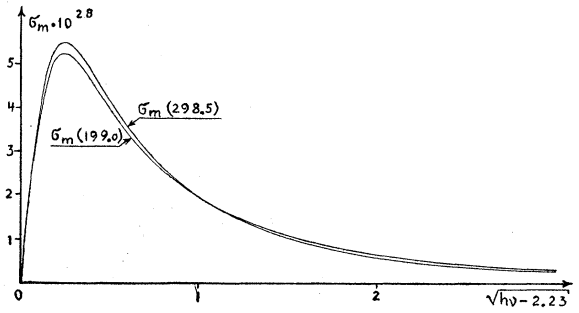

FIG. 3. The photomagnetic cross section as a function of $(h\nu-2.23)^{\frac{1}{2}}$. Two meson masses.

total cross section at γ-energies above 4 Mev seem to favor a meson mass between 250 and 300. There is, however, a certain discrepancy at lower energies which is brought out by Fig. 5. Taking the measurements of Halban and Siegbahn and collaborators,[13] we see not only that the most probable theoretical cross sections fall short of the experimental values but also that the energy dependence is rather different. The results of Snell, Barker, and Sternberg (see caption of Fig. 4, reference b) show the same trend of the cross section

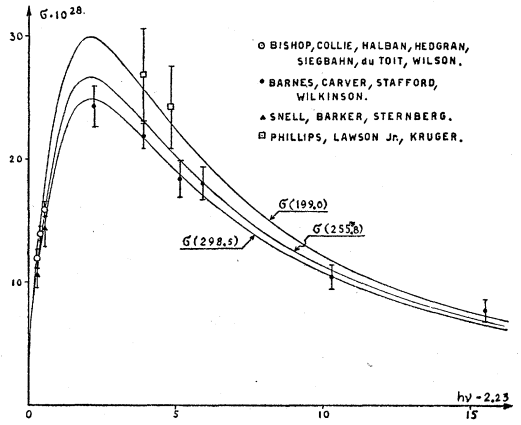

FIG. 4. The total photo cross section as a function of excess energy $h\nu-2.23$. Three meson masses. The following table lists the experimental results and the comparison with the theoretical results for a meson mass $M_m/M_e=286.4$.

$h\nu$ (Mev)	σ_{exp} (10^{-28} cm²)	Ref.	σ_{theor} (10^{-28} cm²)	Ratio $\sigma_{exp}/\sigma_{theor}$
2.504	11.9±0.8	a	9.92	1.20±0.08
	10.6(±1.1)	b		
2.618	13.9±0.6	a	12.18	1.14±0.05
2.757	15.9±0.6	a	14.80	1.07±0.04
	14.3±1.1	b		
4.45±0.04	24.3±1.7	c	25.36	
6.14±0.01	21.9±1.0	c	22.09	
	26.9±3.8	d		
7.0	24.2±3.4	d	19.91	
7.39±0.15	18.4±1.5	c	19.01	
8.14±0.08	18.0±1.3	c	17.33	
12.50±0.21	10.4±1.0	c	10.61	
17.6 ±0.2	7.7±0.9	c	6.68	

[a] See reference 13.
[b] Snell, Barker, and Sternberg, Phys. Rev. **80**, 637 (1950).
[c] Barnes, Carver, Stafford, and Wilkinson, Phys. Rev. **86**, 359 (1952).
[d] Phillips, Lawson, and Kruger, Phys. Rev. **80**, 326 (1950).

[13] Bishop, Collie, Halban, Hedgran, Siegbahn, Du Toit, and Wilson, Phys. Rev. **80**, 211 (1950).

increasing more slowly with energy than is predicted by theory. This tendency was already observed by Halban and Siegbahn and collaborators (see especially their Table IX and Discussion). They also indicated that a better agreement would be obtained if the theoretical photomagnetic cross section were increased, for example, by charge exchange. On the other hand, differences, if any, between later experiments by Bishop, Beghian, and Halban on the angular distribution of photoprotons and the present theoretical values of σ_m/σ_e (see caption of Fig. 6) rather point in the opposite direction. An increase of the theoretical σ_m, sufficient to give agreement with the measured total cross sections, would lead to a definite discrepancy in the angular distribution. Thus, although the experiments discussed here seem very accurate, they do not allow more definite theoretical conclusions.

VIII. THE EFFECTIVE RANGE AND THE PHOTO CROSS SECTIONS

The concept of effective range, originally introduced in the theory of low energy scattering,[14,15] has also been used in the theory of photodisintegration.[16–18] It appears, however, that the accuracy of the resulting cross sections will not be quite satisfactory, unless the effect of the potential shape is taken into account. In particular this applies to the Yukawa potential. Salpeter[17] has already given a thorough general discussion of the shape effects, and it may be of some interest to compare his results for the Yukawa potential with ours.

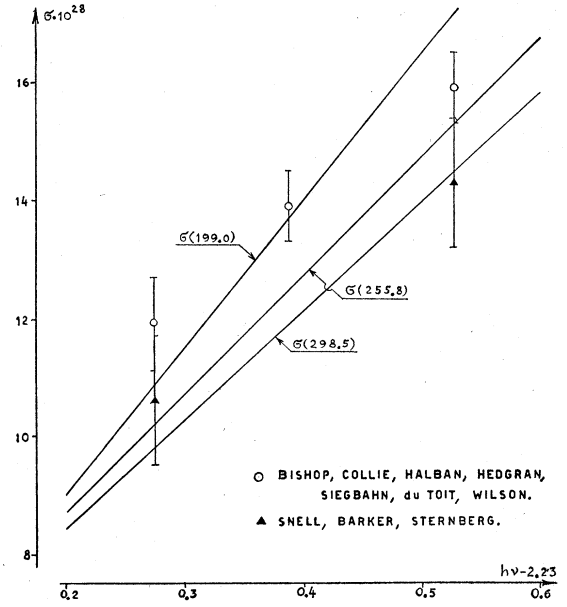

FIG. 5. The total photo cross section as a function of excess energy $h\nu-2.23$ in the interval 0.2–0.6 Mev. Three meson masses.

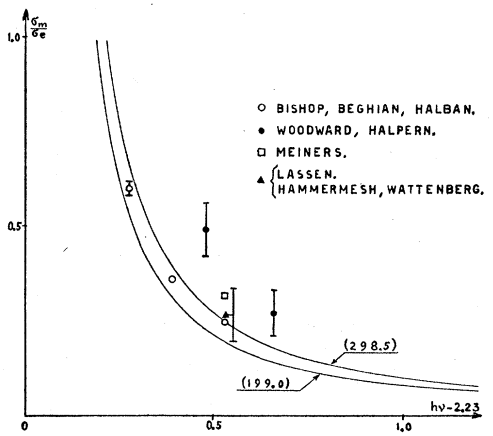

FIG. 6. The ratio of photomagnetic to photoelectric cross section as a function of excess energy $h\nu-2.23$. Two meson masses. The following table lists the experimental results and the comparison with the theoretical results for a meson mass $M_m/M_e=286.4$.

$h\nu$ (Mev)	$(\sigma_m/\sigma_e)_{\text{exp}}$	Ref.	$(\sigma_m/\sigma_e)_{\text{theor}}$
2.504	0.600 ±0.02	a	0.664
2.618	0.360 ±0.008	a	0.386
2.71	0.49 ±0.07	b	0.279
2.757	0.247 ±0.007	a	0.243
	0.317 ±0.012	c	
	0.265 ±0.065	d	
	0.265 ±0.07	e	
2.89	0.27 ±0.06	b	0.176

The result given in reference e has been corrected for γ-ray momentum.

[a] Bishop, Beghian, and Halban, Phys. Rev. **83**, 1052 (1951).
[b] W. M. Woodward and I. Halpern, Phys. Rev. **76**, 107 (1949).
[c] E. P. Meiners, Jr., Phys. Rev. **76**, 259 (1949).
[d] N. O. Lassen, Phys. Rev. **75**, 1099 (1949).
[e] B. Hammermesh and A. Wattenberg, Phys. Rev. **76**, 1408 (1949).

A. Different Integrals Related to the Triplet Effective Range

To begin with, we compute the various integrals $\rho(E_1, E_2)$ (the notation is that of reference 15) for the Yukawa potential. Having fixed the deuteron binding energy and chosen a meson mass, corresponding to a suitable value of $(-a_0)^{\frac{1}{2}}$ [see Eqs. (2) and (3)], we obtain the binding parameter b and the ground state eigenfunction from the tables of Hulthén and Laurikainen[4] (see also Table I above). $\rho(-\epsilon, -\epsilon)$ is then obtained from

$$\rho(-\epsilon, -\epsilon)=1/\kappa[(-a_0)^{-\frac{1}{2}}-2C^{-2}].$$

The normalization constant C [Eq. (3)] has been corrected according to Sec. IV above, which means that the error in $\rho(-\epsilon, -\epsilon)$ does not exceed a few parts in a thousand. The triplet scattering length a_t and effective range $r_t=\rho(0, 0)$ are obtained from Table XII of Hulthén and Skavlem.[6] $\rho(0, -\epsilon)$ is given by

$$\rho(0, -\epsilon)=\frac{2}{\kappa(-a_0)^{\frac{1}{2}}}\left(1-\frac{1}{\kappa a_t(-a_0)^{\frac{1}{2}}}\right).$$

[14] J. M. Blatt and J. D. Jackson, Phys. Rev. **76**, 18 (1949).
[15] H. A. Bethe, Phys. Rev. **76**, 38 (1949).
[16] H. A. Bethe and C. Longmire, Phys. Rev. **77**, 647 (1950).
[17] E. E. Salpeter, Phys. Rev. **82**, 60 (1951).
[18] D. H. Wilkinson, Phys. Rev. **86**, 373 (1952).

TABLE XI. Triplet-scattering length a_t and different integrals related to the triplet-effective range as functions of meson mass. $\epsilon=|E_0|=2.23$ Mev; a_t and ρ in 10^{-13} cm.

$(-a_0)^{\frac{1}{2}}$	M_m/M_e	a_t	$\rho(-\epsilon,-\epsilon)$	$\rho(0,-\epsilon)$	$\rho(0,0)$	$\rho(0,2.5)$	$\rho(0,5)$
0.25	358.2	5.227	1.564	1.510	1.461	1.418	1.385
0.30	298.5	5.350	1.763	1.674	1.599	1.542	1.498
0.35	255.8	5.453	1.940	1.804	1.705	1.633	1.582
0.40	223.9	5.533	2.096	1.904	1.778	1.698	1.644
0.45	199.0	5.589	2.237	1.971	1.823	1.747	1.690
0.3126	286.4	5.377	1.810	1.709	1.629	1.567	1.521

For positive energies $\rho(0, E)$ has been calculated from the formula

$$k\cot\eta=-1/a_t+\tfrac{1}{2}\rho(0,E)k^2,$$

using the asymptotic phases η given by Hulthén and Skavlem. E denotes the energy in Mev in the center-of-mass system: thus $\rho(0, 2.5)$ corresponds to Salpeter's $\rho(0, 5)$. The resulting ρ-values are given in Table XI for six different meson masses. The figures of the last row (interpolated) correspond to the empirical value of $a_t=(5.377\pm0.021)\times10^{-13}$ cm, obtained from $\sigma_0=20.36\pm0.10$ barns, f (coherent scattering amplitude) $=(-3.78\pm0.02)\times10^{-13}$ cm, which gives a meson mass 286 ± 9, assuming $|E_0|=2.230\pm0.004$ Mev. We then have $\rho(0,-\epsilon)=(1.709\pm0.028)\times10^{-13}$ cm (probable error). Thus the uncertainty in the empirical value of $\rho(0,-\epsilon)$ is smaller than the difference between $\rho(0,0)$, $\rho(0,-\epsilon)$, and $\rho(-\epsilon,-\epsilon)$. We also note that the linear dependence of $\rho(E_1, E_2)$ on (E_1+E_2), assumed by Salpeter,[17] is valid only for rather small energies. For example, taking the figures of the last row in Table XI, we need the quadratic formula,

$$\rho(0,E)=\rho(0,0)-0.068\frac{E}{|E_0|}+0.012\left(\frac{E}{|E_0|}\right)^2,$$

to account for the three values $\rho(0,-\epsilon)$, $\rho(0,0)$, and $\rho(0,2.5)$.

B. The Photoelectric Cross Section

The photoelectric cross section may be written[18]

$$\sigma_e=\sigma_{e0}[1-\gamma\rho(-\epsilon,-\epsilon)]^{-1}F^2,$$

$$\sigma_{e0}=\frac{8\pi}{3}\frac{e^2}{\hbar c}\left(\frac{M_n}{M}\right)^2\frac{\hbar^2}{M}\frac{|E_0|^{\frac{1}{2}}(h\nu-|E_0|)^{\frac{3}{2}}}{(h\nu)^3}.$$

σ_{e0} is the expression of Bethe and Peierls, where the ground state wave function is assumed to be $2\gamma^{\frac{1}{2}}e^{-\gamma r}$,

TABLE XII. Parameter E_1 in the correction factor F as a function of meson mass, E_1 in Mev.

$(-a_0)^{\frac{1}{2}}$	M_m/M_e	E_1
0.30	298.5	48.74
0.35	255.8	37.89
0.40	223.9	30.72
0.45	199.0	25.57

TABLE XIII. Correction factor F^2 as a function of energy for two meson masses.

$h\nu$ (Mev)	F^2 $M_m/M_e=298.5$	$M_m/M_e=255.8$
2.23	0.9976	0.9960
4.0	0.9927	0.9884
6.0	0.9847	0.9762
8.0	0.9747	0.9615
10.0	0.9632	0.9450
12.0	0.9507	0.9273
14.0	0.9377	0.9098
16.0	0.9237	0.8912

$\gamma=(M|E_0|/\hbar^2)^{\frac{1}{2}}$. The main error in σ_{e0} is due to the wrong normalization; this is corrected by the factor $[1-\gamma\rho(-\epsilon,-\epsilon)]^{-1}$, while F^2 accounts for the difference between the correct eigenfunction and its asymptotic form. F and $\rho(-\epsilon,-\epsilon)$ depend on the potential shape, F on the energy as well. If $\rho(0,-\epsilon)$ is substituted for $\rho(-\epsilon,-\epsilon)$, as is done in reference 16, the value of σ_e decreases by 4 percent in the case of a Yukawa potential with meson mass 286.

F can be computed as the ratio of the matrix element J_e [Eq. (6)] to a corresponding expression $(J_e)_{\text{asymptotic}}$, where the ground-state function $\phi_0(x)$ has been replaced by its asymptotic form. It appears that F can be accurately[19] represented by the formula

$$F=1-0.640(h\nu/(E_1+h\nu))^2,$$

where E_1 depends on the meson mass [compare the expression of F for the Hulthén potential, reference 18, Eq. (3)]. E_1 is given for different meson masses in Table XII, while Table XIII contains F^2 for a few meson masses and some energies from threshold up to 16 Mev. From Table XIII we conclude that the shape-dependent version of the effective range theory is rather accurate, giving σ_e with an error less than 2 percent up to γ-energies about 6 Mev, if we keep to ranges corresponding to a meson mass above 275 M_e.

C. The Photomagnetic Cross Section

In all calculations of the photomagnetic cross section σ_m based on the effective range theory, the authors have started from the experimental value of σ_c, the capture cross section. On the other hand, in the presentation given above both quantities σ_m and σ_c were calculated

TABLE XIV. Singlet scattering length a_s and different integrals related to the singlet effective range as functions of meson mass. a_s and ρ in 10^{-13} cm.

M_m/M_e	a_s	$\rho(0,0)$	$\rho(0,2.5)$	$\rho(0,5)$
298.5	−23.710	3.023	2.865	2.747
255.8	−23.636	3.582	3.346	3.175
199.0	−23.543	4.749	4.290	3.995
286.4	−23.690	3.162	2.987	2.856

[19] The deviations between F obtained from this formula and F calculated directly do not exceed 0.0005 in the energy interval up to 16 Mev for meson masses 298.5 and 255.8 M_e.

theoretically. Therefore, a direct comparison of the numerical results for σ_m would not tell us so much about the effective range approximation itself.

To get an idea of its accuracy we have first computed the integral $\rho(0, E)$ connected with the singlet state [$\rho(0, 0)=r_s$, the singlet effective range] for a few meson masses and energies. The procedure has already been indicated in Sec. VIIIA, and the results are found in Table XIV.

Secondly, we have calculated the integral D introduced by Bethe and Longmire[16] [Eq. (25)] for various meson masses and energies, using our approximate eigenphases and eigenfunctions. It appears that D can be accurately represented by a linear function of energy up to 5–6 Mev, the variation with energy being small. The results are given in Table XV, together with an interpolation to meson mass 286. For comparison Table XV also includes the D values obtained from the

TABLE XV. The integral D and some approximations to D (see the text) as functions of meson mass. D, D_{BL}, and D_S in 10^{-13} cm. Energy E in Mev.

M_m/M_e	D	D_{BL}	D_S
298.5	$1.120(1-0.0071E)$	1.174	1.113
255.8	$1.265(1-0.0083E)$	1.347	1.230
199.0	$1.530(1-0.0103E)$	1.680	1.413
286.4	$1.158(1-0.0074E)$	1.218	1.145

approximate formula of Bethe and Longmire

$$D_{BL}=\tfrac{1}{4}[r_s+\rho(0, -\epsilon)],$$

and of Salpeter

$$D_S=0.686+0.146r_s+0.57[\rho(0, -\epsilon)-1.720]$$
$$-0.09[\rho(0,-\epsilon)-1.720]r_s, \text{ in units } 10^{-13} \text{ cm}.$$

Finally, we have calculated σ_m by the effective range formula given by Salpeter[17] [Eqs. (22)–(24b)],[20] using the same value for r_s[$=\rho(0, 0)$, Table XIV] but different values of D[D_{BL}, D_S, and D for energy zero, according to Table XV]. The approximation common to these three cases is not only that D is considered independent of energy but also that $k\cot\eta$ is replaced by $-1/a_s+\frac{1}{2}r_sk^2$. Besides, in the BL version we have found it most consistent to use $\rho(0, -\epsilon)$ instead of $\rho(-\epsilon, -\epsilon)$ in the normalization factor. In Table XVI the results are compared with the σ_m values interpolated from our Tables VII and VIII. The difference between the S version and the improved result is due only to the different D values used.

[20] Of course we have other numerical constants in (23) than Salpeter. In (24a) there is a misprint: the expression in the first brackets should be squared.

TABLE XVI. Photomagnetic cross section σ_m calculated according to different effective range versions and values interpolated from Tables VII to VIII.

		$\sigma_m(10^{-28}$ cm)			
		Effective range			Interpolated from Tables VII–VIII
M_m/M_e	$h\nu$ (Mev)	Bethe-Longmire	Salpeter	Improved	
298.5	2.504	3.722	3.988	3.971	3.971
	2.757	2.706	2.908	2.895	2.902
	6.14	0.540	0.602	0.597	0.587
255.8	2.504	3.627	3.995	3.916	3.921
	2.757	2.641	2.926	2.863	2.872
	6.14	0.544	0.642	0.617	0.599

The conclusion is that the shape-dependent effective range approximation can give rather accurate results for σ_m in the most interesting region (up to 6 Mev), provided the calculations are based on an accurate knowledge of the ground state as well as the singlet state of zero energy.

In the present paper no attempt has been made to estimate the influence of noncentral forces. The preliminary discussion of Bethe and Longmire[16] indicates that the influence on the photo cross sections will not be considerable. However, we feel that the increasing accuracy of the experiments may soon make a more detailed study worth while, and we hope that the calculations on the neutron-proton problem with tensor forces which are in progress at this institute will enable us to return to the question on a later occasion.

We are indebted to Mr. Vilhelms Grinvalds for carrying out the greater part of the numerical work. Financial support from the Swedish Atomic Energy Committee and the Swedish State Council of Technical Research is gratefully acknowledged.